

Provided for non-commercial research and education use.
Not for reproduction, distribution or commercial use.



This article appeared in a journal published by Elsevier. The attached copy is furnished to the author for internal non-commercial research and education use, including for instruction at the authors institution and sharing with colleagues.

Other uses, including reproduction and distribution, or selling or licensing copies, or posting to personal, institutional or third party websites are prohibited.

In most cases authors are permitted to post their version of the article (e.g. in Word or Tex form) to their personal website or institutional repository. Authors requiring further information regarding Elsevier's archiving and manuscript policies are encouraged to visit:

<http://www.elsevier.com/authorsrights>



Contents lists available at SciVerse ScienceDirect

International Journal of Plasticity

journal homepage: www.elsevier.com/locate/ijplas

Long range internal stresses in single-phase crystalline materials

M.E. Kassner^{a,*}, P. Geantil^a, L.E. Levine^b^a Aerospace and Mechanical Engineering, University of Southern California, Los Angeles, CA 90089-1453, USA^b Material Measurement Laboratory, National Institute of Standards and Technology, 100 Bureau Drive, Gaithersburg, MD 20899-8553, USA

ARTICLE INFO

Article history:

Received 31 March 2012

Received in final revised form 25 July 2012

Available online 2 November 2012

Keywords:

Long range internal stress

Bauschinger effect

Cyclic deformation

X-ray microbeam

ABSTRACT

Backstresses, or long range internal stresses (LRISs), have been suggested by many to exist in plastically deformed crystalline materials. Elevated stresses may be present in regions of elevated dislocation density or dislocation heterogeneities in the deformed microstructures. The heterogeneities include dislocation pile-ups, edge dislocation dipole bundles and cell walls in monotonically and cyclically deformed materials. The existence of LRIS is especially important for the understanding of cyclic deformation and monotonic deformation. Theories and supporting experiments for assessing LRIS will all be discussed in this review. This review includes several new developments over the past few years.

© 2012 Elsevier Ltd. All rights reserved.

1. Introduction

The applied stress, τ_a , on a crystalline material may not result in a uniform stress across the material. The concept of internal stress generally refers to the deviation of these local stresses from the applied stress. Internal stress fields in crystals can be either short range, such as with individual dislocations in a tilt boundary, or long-range internal stresses (LRIS) which refer to variations in stress that occur over longer length scales, such as that of the microstructure (e.g. dislocation cell size, which is often micrometer-range). LRIS appears to be important for a variety of practical reasons including the Bauschinger effect (as a “backstress”), cyclic deformation, springback in metal forming, as well as, of course, understanding plastic deformation, in general. Certainly, some have been skeptical regarding the existence of substantial long range internal stresses (e.g. Hansen, 1999; Kuhlmann-Wilsdorf, 1999; Neumann, 1999; Kassner et al., 2000; Legros et al., 2008; Sleswyk et al., 1978).

The definition we use for LRIS is:

$$\tau_l = \tau_a + \Delta\tau_i, \quad (1)$$

where τ_l is the local stress, τ_a is the applied stress and $\Delta\tau_i$ is the LRIS. Simply stated, LRIS is the local deviation from the average (or applied) stress in a loaded material. This is illustrated in Fig. 1. Again, these heterogeneous stress states are often suggested to be associated, in single-phase materials, with corresponding heterogeneities in the dislocation substructure such as dislocation pile-ups, subgrain and cell walls and dipole bundles and walls, etc.

This review wishes to describe the history of the LRIS concept in terms of its sources and postulated magnitudes. There has been some controversy as to the existence of LRIS but also wide disagreement as to the magnitude and origin of these stresses in cases where their presence is believed to be confirmed. This discussion of LRIS recognizes that their existence and magnitude may well vary with the nature of the dislocation substructure. We generally consider the principal sources for LRIS in single phase metal and alloys will be dislocation arrangements, and these arrangements vary with both the

* Corresponding author. Address: Department of Aerospace and Mechanical Engineering, OHE 430, University of Southern California, Los Angeles, CA 90089-1453, USA. Tel.: +1 213 453 4119.

E-mail address: kassner@usc.edu (M.E. Kassner).

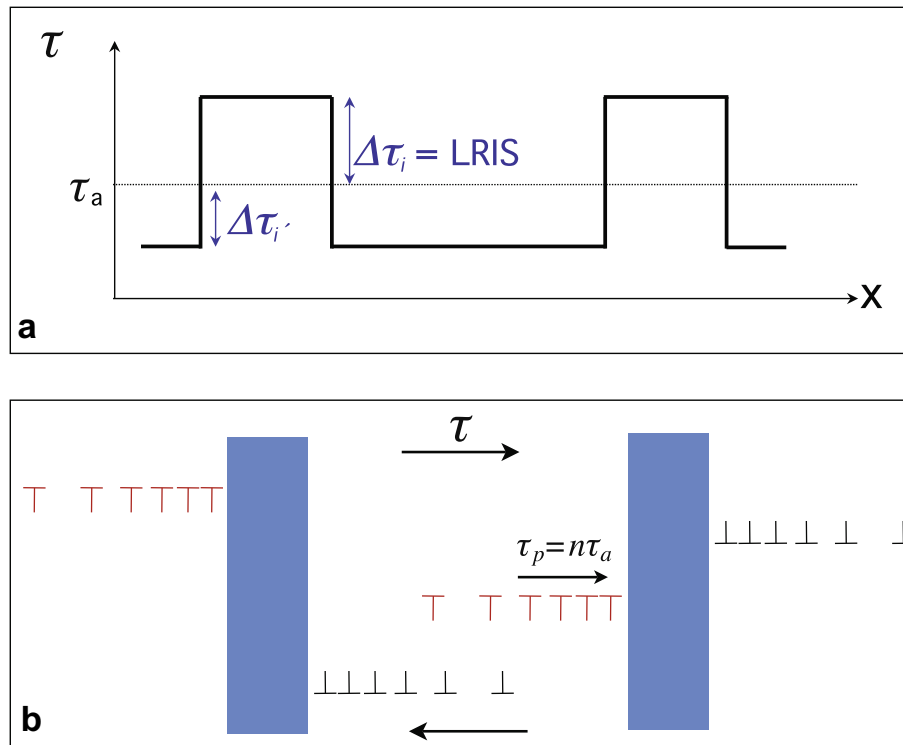


Fig. 1. (a) The variation of stress in a solid with τ_a as the applied stress, and $\Delta\tau_i$ and $\Delta\tau_i$ as the LRIS. Often the heterogeneous stress states are suggested to be associated with corresponding heterogeneities in the dislocation substructure resulting from subgrains, cells and dipole bundles, etc. (b) Idealized dislocation pile-ups against dislocation heterogeneities such as cell walls or grain boundaries. The stress ahead of the pile-up is $\tau_p = n\tau_a$. Equilibrium suggests a equal “backstress” of opposite sign.

temperature and the nature of the deformation. Sometimes there is confusion regarding the presence of LRIS in terms of the dislocations and their arrangements. In pure single crystals, only the dislocations can give rise to LRIS; slip in the absence of dislocations would not give rise to any LRIS.

Two broad categories for deformation are *cyclic* and *monotonic*, with each class producing different kinds of substructure (e.g. in terms of the dipole content of the dislocation heterogeneities and the crystallographic misorientation across these structures). Each of these categories can be further subdivided. Cyclic can be separated by the number of cycles into lower total-cycles, or pre-saturation substructures, and higher total-cycles, or saturated (in terms of the applied stress) structures that often have persistent slip bands (PSBs) or a duplex dislocation structure. The walls of the PSBs are often suggested to have particularly high LRIS. Monotonic is subdivided into low and high (creep) temperature deformation.

In this review, the Bauschinger effect will be discussed first. This, for many, was an early suggestion of “kinematic hardening”, and thus backstresses or long-range internal stresses (LRIS). This section is followed by Monotonic Deformation which is subdivided into low-temperature (generally ambient) deformation and high-temperature deformation. The third section is cyclic deformation which includes pre-saturation and saturation (persistent slip bands or PSBs) microstructures. This subdividing approach allows a discussion of LRIS in terms of the nature of the substructures. This subdivision still suffers from some inconveniences. Different methodologies to assess LRIS (with perhaps different reliabilities) have been applied to the different substructures. There is essentially a matrix of discussions with substructures and the associated experimental methodologies, and (often the subsequent) theories for any LRIS. This means that there is no perfect order for the presentation of data and theories in the background section.

2. Background

2.1. Bauschinger effect

The concept of backstresses or long-range internal stresses in materials may have been first discussed in connection with the Bauschinger effect (Mughrabi, 1987). The material strain hardens and on reversal of the direction of the straining, the metal plastically flows at a stress less in magnitude than in the forward direction, in contrast to what would be expected based on isotropic hardening. A Bauschinger effect is illustrated in Fig. 2. Often a “backstress” is suggested based on the equation (Kassner et al., 1985; Yan, 1998)

$$\sigma_b = (\sigma_f + \sigma_r)/2, \tag{2}$$

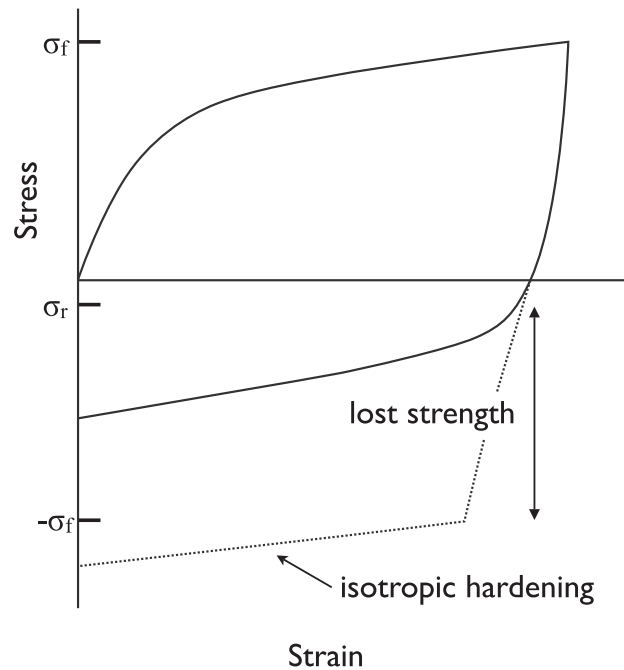


Fig. 2. A generalized description of the Bauschinger effect.

where σ_b is the “backstress” (which is often referred to or related to LRIS by other investigators, but as discussed subsequently, this may not be true), σ_r is the stress of yielding on reversal of the direction of straining, and σ_f is the stress (forward sense) just prior to the reversal. Backstresses have sometimes been thought of as the origin of kinematic hardening (or a translation of the yield surface). With $\sigma_b = 0$, there is no backstress and all hardening is isotropic. With immediate yielding on reversal, $\sigma_b = \sigma_f$ and all hardening is kinematic. Not only is the flow stress lower on reversal but the hardening features are very different, as well, from the forward sense. The Bauschinger effect is important as it appears to be the basis for low hardening rates and low saturation stresses (and failure stresses) in cyclic deformation (fatigue). This is shown (later) in Fig. 4.

2.1.1. Pile-up model of the Bauschinger effect

One of the early physically-based explanations for the Bauschinger effect was that dislocation pile-ups, illustrated in Fig. 1b, lead to LRIS (Seeger et al., 1957). The stress, τ_p , ahead of the pile-ups is estimated by,

$$\tau_p = n\tau_a, \quad (3)$$

where n is the number of dislocations in the pile-up (Weertman and Weertman, 1992). Thus, with the presence of pile-ups, high local stress develops. For local equilibrium, the high stress against a barrier (e.g. cell walls), τ_p , would be balanced by a stress, $-\tau_p$. Seeger et al. (1957) and Mott (1952) suggested that on reversal of the direction of straining, this internal stress, $-\tau_p$, assists the reverse plasticity and decreases the corresponding applied stress.

2.1.2. Composite model of the Bauschinger effect

In an influential development, Mughrabi (1983) and Pedersen et al. (1981) independently advanced the concept of relatively high (long-range internal) stresses in association with heterogeneous dislocation substructures (e.g., cell/subgrain walls, dipole bundles, PSB walls, etc.) through a “composite” model. Mughrabi presented the simple case where “hard” (high dislocation density walls, etc.) and “soft” (low dislocation density channels, or cell interiors) elastic-perfectly-plastic regions are compatibly sheared. Each component yields at different stresses (depending on the dislocation density and arrangements) and it is suggested that the composite is under a heterogeneous stress-state with the high-dislocation density regions having the larger magnitude stress. Thus, LRIS are present consistent with Fig. 1a.

This composite picture was suggested to explain the Bauschinger effect. As soft and hard regions are unloaded in parallel from tension, the hard region eventually places the soft region in compression while the stress in the hard region is still positive. When the applied, or average, stress is zero, the stress in the hard region is positive while negative in the soft region. A Bauschinger effect is observed, where plasticity occurs on reversal at a lower average magnitude of stress than just prior to unloading due to “reverse” plasticity in the soft region. The “composite” model for backstress is illustrated in Figs. 3 and 4. The long range internal stresses are defined consistent with Eq. (1), $\tau_w^y = \tau_a + \Delta\tau_w$ and $\tau_i^y = \tau_a + \Delta\tau_i$, where τ_a is the applied stress, and $\Delta\tau_w$ and $\Delta\tau_i$ are LRIS in the cell wall and cell interior of the composite substructure. The concept of heterogeneous stresses has also been widely embraced for monotonic deformation (Borbély et al., 1997, 2000; Vogerand and Blum, 1990) including elevated-temperature creep deformation.

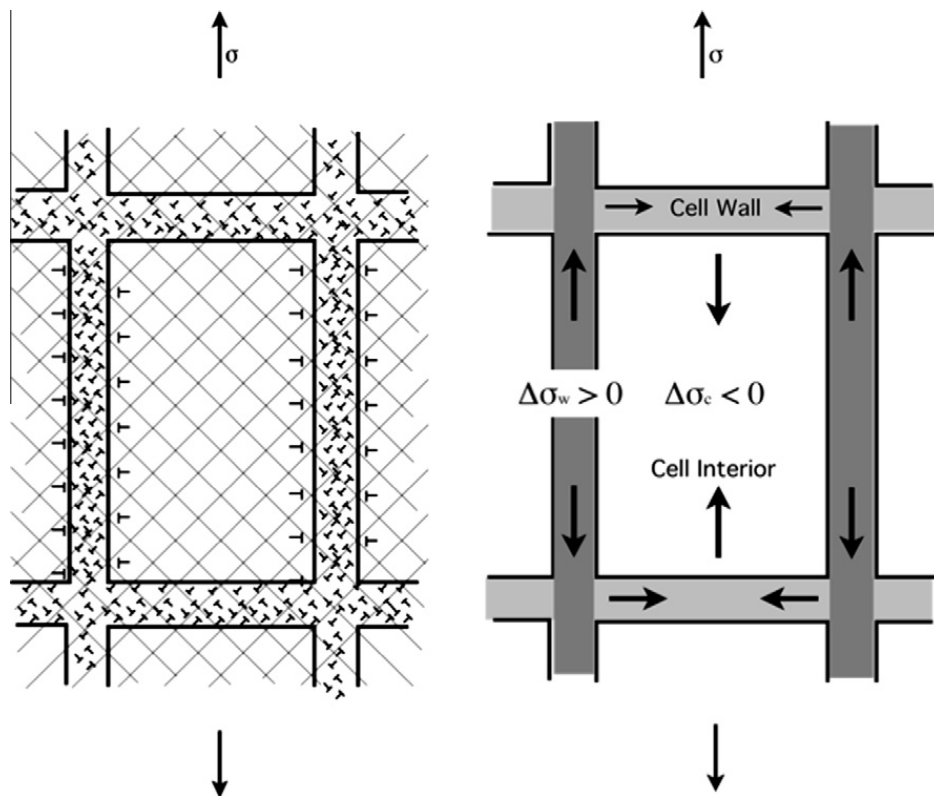


Fig. 3. The composite model indicating “hard” regions (high dislocation density) and “soft” regions (low dislocation density). Note that interfacial dislocations at the interface allow elastic compatibility and form dipole pairs across the walls.

Note that the yield stress on reversal is related to the LRIS in the composite, but σ_b of Eq. (2) is not equal to the LRIS. Also note that elastic-perfectly-plastic behavior is assumed as well. As Mughrabi points out, the disparate stresses suggest an elastic incompatibility and further suggest the necessity for dislocations at the interface. Of course, the LRIS must ultimately result from the stress-field summations of all of the dislocations in a single-phase material. Said another way, the stress-states (LRIS) of each element in the structure can be, in principle, assessed based on the knowledge of the precise location of all dislocations. The interfacial dislocations in this model are the principal basis for the LRIS.

2.1.3. Non-LRIS explanation for BE

In early work performed by Kassner et al. (1985) a nearly random dislocation arrangement (absent of subgrain and easily discernable cell walls) in monotonically deformed stainless steel produced nearly the same elevated temperature Bauschinger effect as one with well-defined cells and/or subgrains where LRIS could be significant according to the composite model (Kassner et al., 1985). This is illustrated in Fig. 5. Also, it can be noted from the single crystal aluminum experiments of Kassner et al. (1997) and Kassner and Wall (1999) that a very pronounced Bauschinger effect is evident in the first cycle (just 0.0005 monotonic plastic strain) at 77 K when a cellular substructure is not expected to be evident during the very early Stage I deformation (Schmid factor = 0.5). The Bauschinger effect is comparable to the case where a heterogeneous vein/channel substructure developed after hundreds or thousands of cycles. These experiments suggest that the Bauschinger effect is largely independent of such pronounced heterogeneities as cells or subgrains. Inasmuch as LRIS are related to such heterogeneities, perhaps the Bauschinger Effect does not measure nor is especially reflective of LRIS.

Sleeswyk et al. (1978) analyzed the Bauschinger Effect in several metals at ambient temperature. They found that the hardening behavior on reversal can be modeled by that of the monotonic case provided a small (e.g., 0.01–0.05) “reversible” strain is subtracted from the early plastic strain associated with each reversal (in Fig. 6 this is approximately β). This led to the conclusion of an Orowan-type mechanism (long-range internal stresses are not especially important) (Orowan 1959) with dislocations easily reversing their motion (e.g. across cells from dislocation tangles or reversing from pile-ups). Sleeswyk et al. (1978) suggested gliding dislocations, during work hardening, encounter increasingly effective obstacles and the stress necessary to activate further dislocation motion or plasticity continually increases (work-hardening). On reversal of the direction of straining from a “forward” sense, under σ_f , the dislocations will easily move past those, non-regularly-spaced, obstacles that have already been surmounted. Thus, the flow stress on reversal is initially relatively low, $< \sigma_f$. There is a relatively large amount of plastic strain on reversal to $[-(\sigma + d\sigma)]$ in comparison to the strain associated with an incremental increase in stress to $[(\sigma + d\sigma)]$ in the forward direction. This is referred to as the Orowan–Sleeswyk (OS) explanation for the Bauschinger effect. There is the implication that the obstacles to the gliding dislocations are non-uniformly distributed in the slip planes,

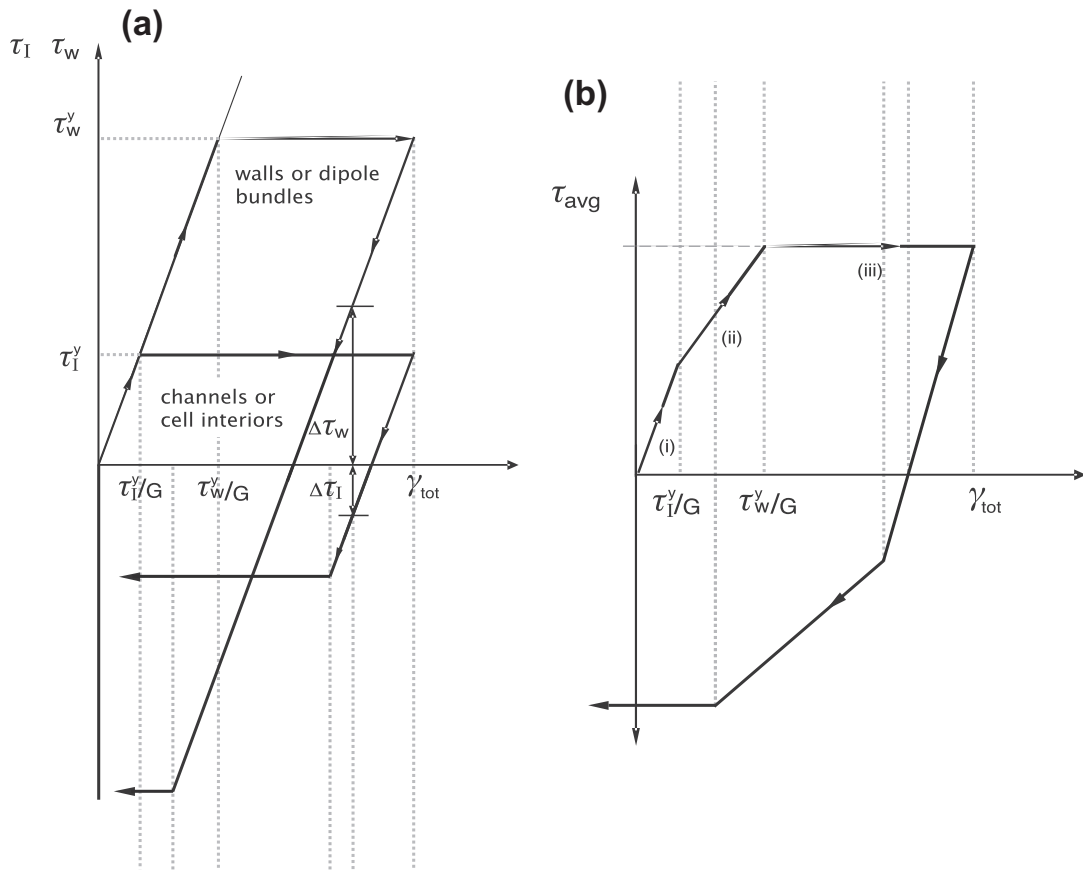


Fig. 4. The composite model illustrating the Bauschinger effect. The different stress versus strain behaviors of the cell walls and the cell interiors are illustrated in (a), while the stress versus strain behavior of the composite is illustrated in (b). When the composite is completely unloaded, the low-dislocation density cell interior region is under compressive (back) stress. This leads to a yielding of this “softer” component in compression at a “macroscopic” stress less than $-\tau_w^y$.

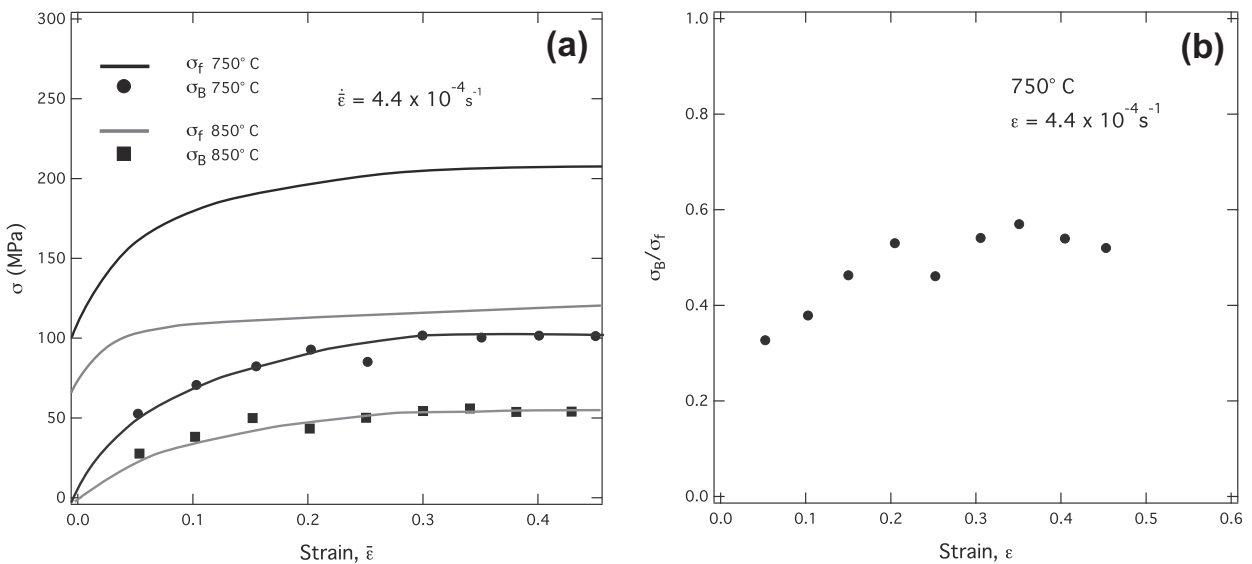


Fig. 5. (a) The backstress defined and calculated by Eq. (2) of 304 stainless steel at creep temperatures, as a function of monotonic strain. (Kassner et al., 1985) and (b), the normalized backstress as a function of strain.

which is expected. An example is cell interiors having a relatively low obstacle density, while cell-walls, dislocation tangles, etc. have a (much) higher density. Sleswyk et al. (1978) suggested that the reversible strain, β , maybe related to the cell size; dislocations have a lower obstacle density on reversal into the cell interior from cell walls where the obstacle density

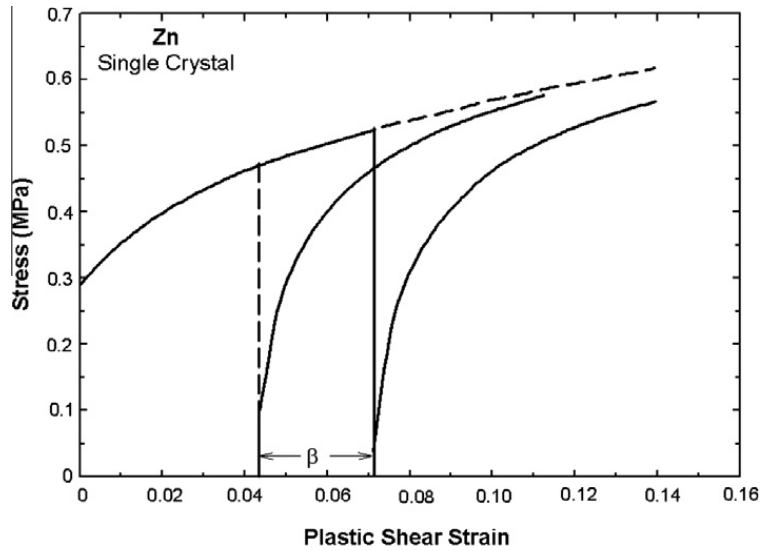


Fig. 6. A zinc single crystal is deformed at ambient temperature in tension to a strain of .07, then unloaded from 0.54 MPa and compressed (although only the magnitude stress is reported in the figure and is always positive in sign). The material yields at $\cong 0.1$ (negative) MPa and gives rise to a Bauschinger effect. The hardening on reversal approaches that for continued monotonic deformation if a “reversible” strain β is subtracted to the dashed vertical line (from Sleswyk et al., 1978).

is higher in the forward sense. This suggests that a substantial component to the Bauschinger effect or the reversible strain, β , is configurational, rather than a “back(ward)” stress from heterogeneities.

Other sources (γ_{NC}) for Bauschinger effect or “reversible” strain (β) on reverse loading include, but are not restricted to: dislocation loop unbowing and re-bowing in the opposite sense (γ_A), plasticity associated with any backstress (LRIS) of opposite sign to the strain prior to unloading (γ_B), recovery on reversal (e.g. recovered plastic strain due to dislocation annihilation) including subgrain boundaries in creep (Kassner et al., 1994a,b; McQueen et al., 1993) (γ_C). These terms could rationalize anelasticity in unloading. Observations of anelasticity in single crystals of 6×10^{-4} (Gibeling and Nix, 1980) and polycrystals of 10^{-3} (Thiehsen et al., 1993a,b) have been observed in unloaded specimens, at temperature, during creep.

A maximum (anelastic) unbowing for a “cubic grid” of dislocations (all bowed to semi-circular configuration) can be estimated as

$$\gamma_A \cong \frac{\pi b}{8} \frac{\sqrt{\rho}}{\sqrt{6}} \quad (4)$$

If $\rho \cong 10^{14} \text{ m}^{-2}$ to 10^{15} m^{-2} for cyclically and monotonically deformed Cu single crystals (Kassner et al., 2000; Levine et al., 2011), an “upper limit” for (γ_A) is 10^{-3} . Not surprisingly, these bowed (“flexing”) dislocations also can give rise to apparent decreases in the elastic modulus during strain-rate increase tests in heavily deformed material (Kassner, 1989).

The backstrain associated with the LRIS (γ_B) is at least σ/E (elastic component), and may be even larger if backstrains (anelasticity) are considered that are activated by the LRIS, in the absence of any relaxation of the LRIS. (γ_C) cannot be easily predicted; this is a contribution to β based on dislocation density changes that are not associated with a relaxation in the LRIS. An example of this could be the recovery of subgrain boundaries at elevated temperature that could give rise to a back-strain. The sum, $\gamma_e + \gamma_A + \gamma_B$, is not readily calculated, but if it is assumed that (γ_B) is roughly σ/E for cyclic and monotonic deformation of Cu, then this sum is roughly 10^{-3} to 3×10^{-3} . The observed values of β are, then, about an order of magnitude too large. Thus, it appears the low proportional limit might be influenced by LRIS and/or anelastic behavior, but the principal features of the Bauschinger effect may need to include the Orowan–Sleswyk type of explanation in addition to any “early” (micro-)yielding from any LRIS. *In situ* reverse deformation experiments in the high voltage transmission electron microscope (HVEM) by Kassner et al. (1991) on pure Al with dislocation tangles, suggested that on reversal, the cell wall formed in monotonic deformation shows some “unraveling”, consistent with the OS explanation. The assistance by LRIS in the unraveling is unclear.

2.2. Monotonic deformation

The same basis for the Bauschinger effect has been suggested for LRIS in monotonically deformed materials (e.g. composite and pile-up models), and several dislocation models have been proposed to rationalize LRIS observations (Khan et al., 2004; Sedlacek et al., 2002; Gibeling and Nix, 1980; Vogerand and Blum, 1990). The experiments described below offer possible justifications for these models.

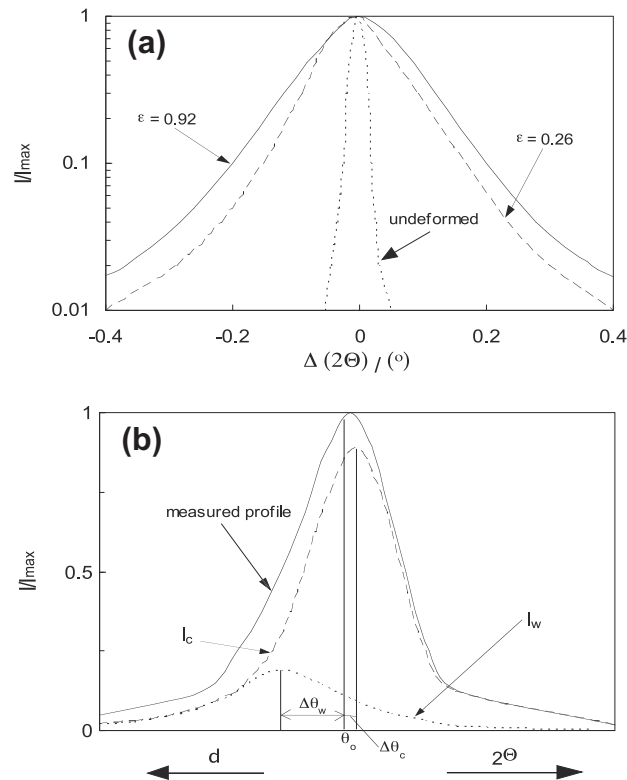


Fig. 7. The X-ray diffraction peak in Cu deformed to various monotonic strains showing asymmetric broadening. A decomposition can be performed that leads to two symmetric peaks which has been interpreted as a heterogeneous stress-state (Schafler et al., 2005), with different lattice parameters (stresses) in high and low dislocation density regions of the plastically deformed material. In this case, LRIS in cell walls were suggested to be about $0.4\sigma_A$ and $0.1\sigma_A$ for cell interiors.

2.2.1. X-ray peak asymmetry

As materials are plastically deformed, the diffraction peaks both broaden and become increasingly asymmetric, as illustrated in Fig. 7. Sophisticated models describing how dislocations produce these peaks have been used to assess dislocation densities, and ratios between screw and edge dislocations (Pedersen et al., 1981; Groma, 1998; Krivoglaz and Ryaboshapka, 1963; Wilkins, 1970; Ungar et al., 1984). The details of the shapes of the peaks have also been used to assess LRIS.

As discussed earlier, it has been argued that a heterogeneous dislocation microstructure can be associated with long range internal stresses (LRISs), often through a two-phase composite model, as illustrated in Fig. 1. If correct, the high and low dislocation volumes would have different stresses, leading to the separation of the diffraction peak into two approximately symmetric subpeaks (Mughrabi and Ungar, 2002). The areas under the subpeaks reflect the corresponding relative volumes. It is usually assumed that the smaller symmetric peak, illustrated in Fig. 7(b), is associated with the high-dislocation volumes such as the cell, PSB or subgrain walls. A review of the literature relating to X-ray line-profile asymmetry experiments shows consistent patterns:

(i) *Asymmetry increases with applied stress and strain*

X-ray line profiles tend to become more asymmetric as the specimen accumulates plastic strain.

(ii) *Characteristic asymmetry*

When comparing asymmetry from the axial to side faces, the asymmetry is in the opposite “sense” or direction, as the composite model predicts due to the Poisson effect.

Thus, the asymmetry is explained by the different lattice parameters (strains) in the composite and the average LRIS from the individual components is assessed through a decomposition process. The single crystal Cu compression deformation experiments by Ungar et al. (1991) suggested relatively low values by this technique at $+0.10\sigma_A$ in the cell interiors and $-0.4\sigma_A$ in the cell walls (Ungar et al., 1991). Although these experiments are indirect, they have been used to infer local stresses based on the irradiation of millions of cells. A recent microbeam diffraction study (Levine et al., 2012) directly tested the validity of this asymmetric peak decomposition process and found that most of the underlying assumptions were true and that the extracted stresses were qualitatively correct.

2.2.2. Synchrotron X-ray microdiffraction experiments

In 2002, Larson et al. (2002) developed a polychromatic X-ray technique, white-beam differential-aperture X-ray microscopy (DAXM), that allows measurement of the crystallographic orientation and the internal deviatoric (shear) stress state in

relatively small, spatially-resolved volumes within a bulk specimen (Larson et al., 2002). These experiments use the micro-beam diffraction instrument on sector 34ID at the Advanced Photon Source at Argonne National Laboratory. More recently, this technique has been extended by using a scanned monochromatic X-ray beam (Levine et al., 2006) to allow absolute lattice parameters and dilatational strains to be measured from buried submicrometer sample volumes. The 3D submicrometer ($\approx 0.5 \mu\text{m}$)³ sample volume of this new technique is small enough to allow probing within individual dislocation cells within a bulk deformed specimen. In scanning-monochromatic DAXM, a submicrometer X-ray beam is scanned through a broad enough range of energies to ensure diffraction from all of the sample volumes along the beam path. For a given photon energy, X-rays diffracted by the dislocation cells are measured using an area detector. A Pt wire is then translated parallel to the sample surface and the locations of the diffracting cells can be determined with submicrometer accuracy. Since the energy (and thus the wavelength) is known, absolute lattice parameters can be obtained. This process is repeated over a wide range of photon energies (up to 600 eV range for 3 eV steps) and a series of lattice parameter values can be assigned to specific, small, volumes of material leading to measurements of the average lattice parameter within individual dislocation cell interiors. Further enhancements to this technique allowed complete diffraction line profiles to be measured from numerous individual, adjacent dislocation cell walls and cell interiors (Levine et al., 2011).

The scanned-monochromatic DAXM technique was first applied to make direct measurements of the strain-state within dislocation cells in deformed copper. Copper single crystals with $\langle 001 \rangle$ orientations were deformed in both tension and compression to strains of $\approx 30\%$ that led to well developed dislocation cell structures such as in Fig. 8.

The deformation-induced change in the lattice parameter reverses sign in tension and compression (negative in tension, positive in compression as measured locally by DAXM). Also, (006) volume average X-ray line profiles, from tension and compression deformed samples were found to contain asymmetry, and the asymmetry “sense” was reversed when comparing tension and compression samples. This is shown in Fig. 9. These two results, when taken together, are direct evidence that a long range internal stress (LRIS) remains after plastic deformation, specifically showing that cell interiors are under compressive stress after tensile deformation and vice versa. Further, these two results are in qualitative agreement with the predictions of the composite model proposed independently by Mughrabi and also by Pedersen. This also suggests that a Mott-Seeger type (pile-up) model for LRIS is unlikely as such a model is not expected to show that stress reversal changes the sign of LRIS. Again, it is important to emphasize that there appears to be a range of values (order of magnitude) for the lattice parameter changes from one cell to the next.

It should be mentioned that the microbeam studies were performed on unloaded specimens and recovery of LRIS must be considered. Borbély et al. (2000) made X-ray peak asymmetry measurements similar to Fig. 7 *in situ*, or under load. The XRD line profiles provided the expected asymmetry under stress at elevated temperature. Additionally, the *unloaded* specimen retained a majority of the asymmetry despite elevated temperature exposure that would lead to recovery of any LRIS. Since it appears that the asymmetry under load is reflective of LRIS, then unloaded specimens appear to substantially “lock in” at least two-thirds of these stresses in Cu at room temperature. Additional experiments to validate these results should be performed.

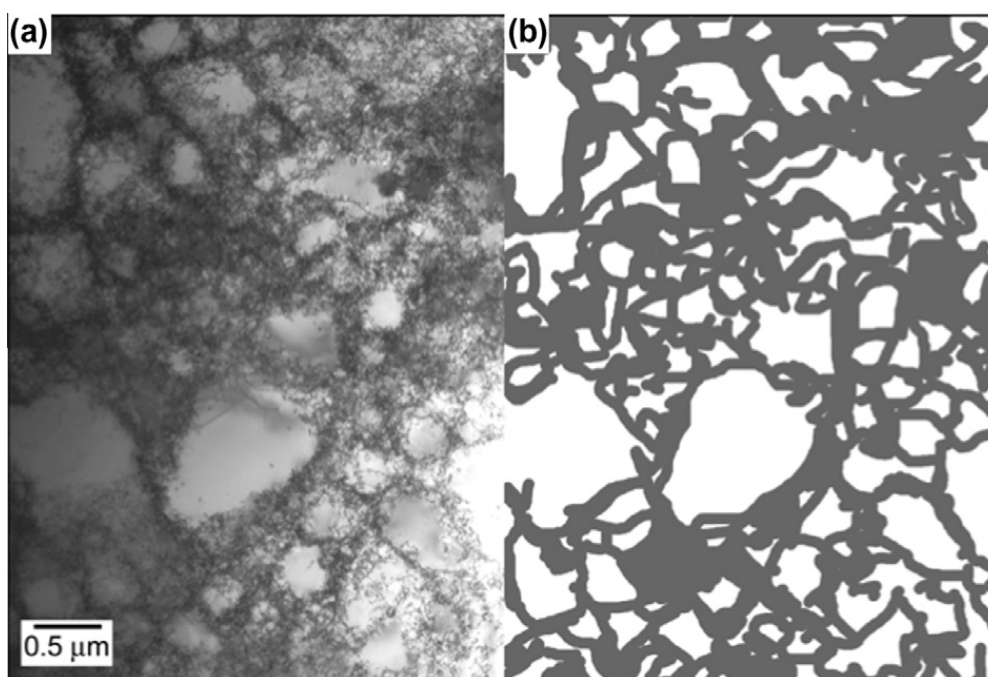


Fig. 8. (a) TEM micrograph of the dislocation substructure of deformed $[001]$ -oriented Cu single crystals compression deformed to a true strain of -0.28 . (b) The same micrograph with the dislocation walls shaded in grey. The shaded area comprises $\approx 55\%$ of the micrograph.

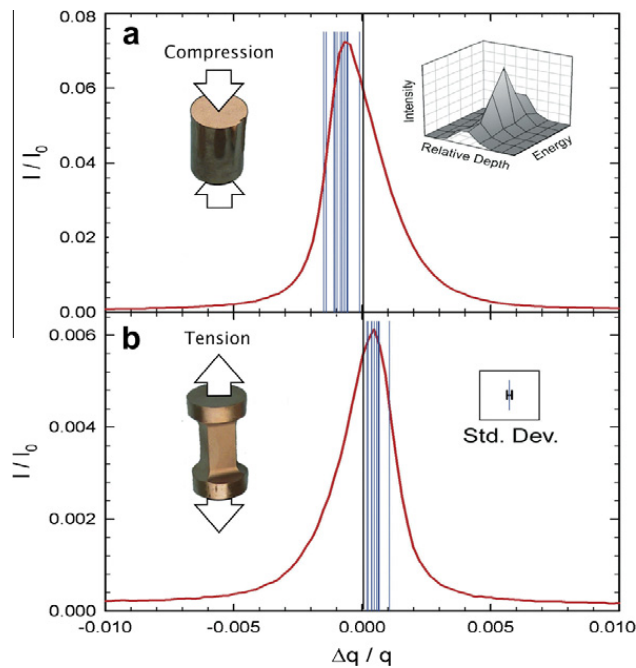


Fig. 9. Comparison between spatially integrated and spatially resolved X-ray diffraction experiments on deformed copper single-crystals. (a) Photograph and X-ray results from the $\langle 001 \rangle$ compression specimen. Inset: a representative beam energy and depth scan for a typical dislocation cell, where the Energy grid lines denote 2 eV steps, the depth grid lines denote 0.5 μm steps and the center of the peak determines the 006 Bragg angle for the cell. (b) Photograph and corresponding results from the $\langle 001 \rangle$ tension specimen. The red lines in both panels are spatially averaged axial 006 line profiles obtained using conventional X-ray diffraction techniques. The vertical blue lines in both panels show the corresponding diffraction peak centers from individual dislocation cells, measured using spatially resolved monochromatic differential-aperture X-ray microscopy. The error bar indicates one standard deviation. As predicted by the two-component composite model, the cell strains in (a) are shifted to smaller q and those in (b) are shifted to larger q . (For interpretation of the references to color in this figure legend, the reader is referred to the web version of this article.)

More recent Cu compression tests, similar to those just discussed, confirm these findings and are illustrated in Fig. 10. However, in these experiments, a large number of the strains from individual cell walls in addition to cell interiors were measured. Unlike the experiments of Fig. 7, where the LRIS are deduced from the decomposition of an X-ray line profile into symmetric sub-peaks, here direct lattice parameter measurements are taken from individual cell walls and cell interiors. The average stress in the cell walls and cell interiors is roughly equal. TEM observations reveal that the cell wall and cell interior volumes are also roughly equal, indicating a balance of forces in the unloaded specimens.

The elastic strains within the cell walls and cell interiors measured have an approximate 40 MPa difference between their averages and are of opposite sign. Thus, the LRIS for both cell walls and cell interiors is roughly 0.1 the applied stress. So, the average value of the LRIS in these specimens is not very large. Of course, it should be mentioned that there is considerable variation from cell wall/interior to the next and a local cell wall, for example can have a local stress that approaches 0.4 the applied stress; the microbeam is well suited to detect these variations, obscured with earlier techniques. Also, note that the magnitude of the LRIS at an average of about ± 20 MPa is significant and it is unclear how the value changes with the flow stress. That is, how this value might change with the flow stress during hardening.

Additionally, there is a broad asymmetric shape to the stress distribution functions shown. A simple model was developed by Levine et al. (2011). It is suggested that the long range internal stress fields of the dislocations within the walls are shielded and that the LRIS are a consequence of the interfacial dipoles illustrated in Fig. 3. The analysis further suggested that the average number of interfacial dislocations needed to create the observed LRIS was very small, only about two, or so, per cell wall.

It must be mentioned, here, that the cell walls examined are typical of those produced by deformation in single crystal Cu along $[100]$. The cells are well-organized and consistently of low misorientation. In off- $[100]$ axis single crystals, where high misorientation boundaries (geometric necessary boundaries or GNBs) are formed, the LRIS could increase over this simple case. Also, care must be exercised in converting strains to stresses. Multiplication of the strain and modulus gives proper stress only if the full strain tensor is known. Future work by the microbeam group will include an evaluation of the full strain tensor.

There is actually reasonable agreement between Levine et al. (2011) Cu monotonic deformation results and the work of Mughrabi et al. (1986) as corrected in Ungar et al. (1991) provided the proper adjustments are performed. Estimates for the volume fractions of cell walls at 0.28 ± 0.001 strain in $[001]$ oriented Cu is actually $f_w \cong 0.55 \pm 0.1$ based on a fairly simple image analysis of TEM micrographs that partition “high” and “low” dislocation density regions. We expect that the cell wall estimates of LRIS of the Mughrabi et al. (1986) (again, as corrected by Ungar et al. 1991), of $0.4\sigma_A$ is based on an assessment

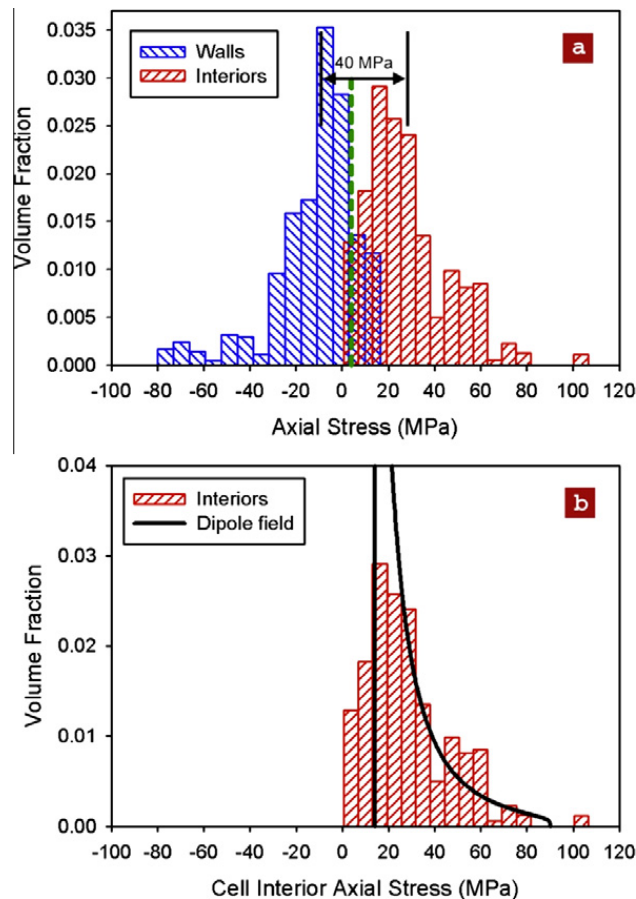


Fig. 10. (a) Measured stress distributions for cell interiors (red) and cell walls (blue). The average sample stress of 4 MPa (dashed green line) is within the measurement uncertainty (7 MPa) of zero. (b) A theoretical stress distribution function from a dipole field model (black curve) is compared with the measured distribution for cell interiors (red). The dipole field model is consistent with the measured results (Levine et al., 2011). (For interpretation of the references to color in this figure legend, the reader is referred to the web version of this article.)

of a very large number of cells are in reasonable agreement with the Levine et al. (2011) work if a more realistic estimate of the volume fraction of walls is used in the Mughrabi et al. work.

2.2.3. Creep

Various models have been suggested to be the basis of LRIS in creep. These include “flexing” subgrain walls (Argon and Takeuchi, 1981; Gibeling and Nix, 1981) leading to backstresses about eight times the applied stress, backstresses from pile-ups (Kassner, 2009) and, of course, the composite model. Below are some of the experimental observations of LRIS or their absence.

2.2.3.1. CBED. Convergent beam electron diffraction (CBED) experiments were used by Kassner et al. (2000, 2002) to assess internal stresses in unloaded monotonically and cyclically deformed Cu. CBED, with a 20–100 nm beam size, can probe smaller volumes than the X-ray studies referenced thus far. Convergent beam electron diffraction experiments were performed near cell/subgrain walls (within 80 nm) and interiors in creep deformed Cu and Al. These experiments measured the lattice parameters in small volumes in various locations in a TEM thin foil. No evidence for LRIS was observed. The uncertainty, however, was 1.5–2.0 times the flow stress for Cu and Al, respectively. These suggest that the LRIS in these creep deformed materials is not very high, if at all present. Of course, the CBED experiments are performed on unloaded material, and the foil thickness is relatively small in the regions examined and relaxation of LRIS is possible. This kind of experiment was also performed on cyclically (fatigued) deformed Cu, later illustrated in Fig. 13.

2.2.3.2. In situ. Morris and Martin (1984) quenched a creep-deformed solid solution Al–Zn alloy that behaves essentially identically to pure Al at elevated temperature. These results are illustrated in Fig. 11. On cooling to ambient temperature however, precipitates form that allegedly pin dislocations (and dislocation loops) in place. The Orowan bowing equation was applied to assess the stresses required for bowing and suggested enormous LRIS near walls. Nabarro et al. point out (Nabarro and de Villiers, 1995), however, that the curvature of the dislocation segments may not reflect just the LRIS but, rather, the curvature was increased by the “chemical pressure” of the super-saturated zinc. The meaning of this criticism

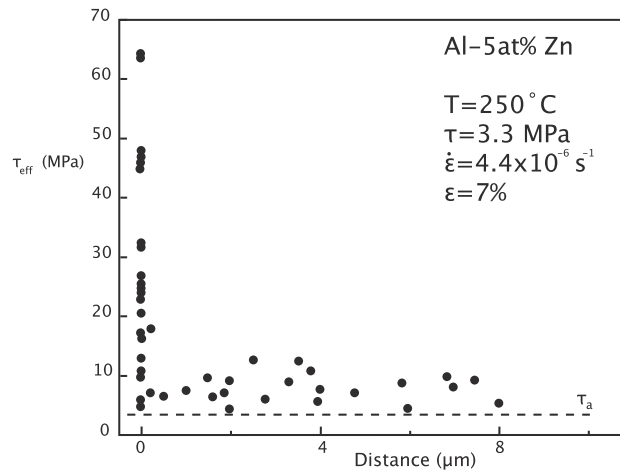


Fig. 11. Dislocation loop-radii-calculated LRIS based on precipitate-pinning (under load) of dislocation loops in creep deformed Al–Zn alloy with subgrains. The high stresses are very close to the subgrain walls. From (Morris and Martin, 1984).

is unclear, but may imply that with low-temperature precipitation, stress fields from the precipitate (coherency or dilatational), or the mass transfer from the matrix to the precipitate (leaving vacancies behind) that may create a hydrostatic stress gradient, leaving bowed dislocations whose configuration is independent of LRIS.

2.2.3.3. X-ray peak asymmetry. Borbély et al. (2000), as mentioned previously, observed X-ray peak asymmetry in creep-deformed Cu under load. Their analysis suggests that LRIS in the walls is about equal to the applied stress. Also Blum, one of the co-authors, increased this value to about 5–7 times the applied stress (Blum, 2012; Vogerand and Blum, 1990). A complication to the analysis is assessing the volume fraction associated with subgrain/cell walls.

Table 1 illustrates the LRIS values from various studies, many already discussed. The table indicates a wide variation of experimental estimates and theoretical predictions for LRIS in deformed materials.

2.3. Cyclic deformation

2.3.1. Saturation (PSBs)

2.3.1.1. In situ experiments for saturation. In situ deformation experiments in the TEM by Lepinoux and Kubin (1985) and particularly the neutron irradiation experiments by Mughrabi (1983) of Fig. 12 have long been cited as evidence for long-range internal stresses in cyclically deformed metals. The observed stresses are, roughly, a factor of three higher than the applied stress for dipole walls in Cu persistent slip band (PSB) walls (i.e., LRIS is about twice the applied stress). These two studies assessed LRIS by measuring dislocation loop radii as a function of position within the heterogeneous microstructure in cyclically deformed Cu single crystals and applying the standard bowing equation:

$$\tau = \frac{Gb}{2r} \quad (5)$$

(Of course, derivation of this equation assumes knowledge of the dislocation core energy and, thus, cannot be regarded as a precise equation.) Recent work by Mughrabi and Pschenitzka (2005) suggests that the actual values may be half his earlier estimates. This is because the connection between the “pinned” dislocation configurations and the elastic strains in the lattice is not as straightforward as Eq. (5), especially since interactions with dipoles and multipoles of the wall are considered important and Eq. (5) is not applicable. Mughrabi’s recent correction is also illustrated in Fig. 12. Nonetheless, it turns out that the case of cyclic deformation to saturation, where PSBs may form, may constitute a case where LRIS are relatively high, at $1.0 \sigma_A$ in comparison to other deformation modes and microstructures. As will be discussed later, other heterogeneities appear to have lower values of LRIS. Lepinoux and Kubin (1985) performed *in-situ* deformation experiments (under load) on Cu with PSBs and also calculated the stress using Eq. (5) and estimates of LRIS are similar to the original values of Mughrabi et al. in Fig. 10, but would suffer the same limitations as the original Mughrabi estimates.

2.3.1.2. X-ray peak asymmetry measurements in cyclic deformation to saturation. Some indirect evidence for internal stresses based on X-ray diffraction (XRD) experiments during cyclic deformation is now discussed that complements earlier X-ray work for monotonic deformation (Mughrabi, 1983; Mughrabi et al., 1986; Mughrabi and Ungar, 2002; Borbély et al., 1997, 2000; Hecker et al., 1997; Biermann et al., 1993; Jakobsen et al., 2006; Pantleon et al., 2004). Basically, X-ray peaks have generally been observed to broaden asymmetrically with plastic deformation. A decomposition can be performed on the asymmetric peak profile into two, usually, assumed symmetric peaks; one peak is suggested to represent the material in the vicinity of the high dislocation-density heterogeneities such as dipole bundles, persistent slip bands (or PSB dipole

Table 1
Selected studies of long-range internal stresses.

Mat.	Ref.	Deformation mode	Strain	LRIS (σ_A)		Observation method	Temp.	Notes
				Walls	Interior			
Cu	Mughrabi and Pschenitzka (2005) and Mughrabi (1983)	Cyclic	Saturation w/ PSBs	+1.0	-0.37	in-situ neutron irradi.	RT	reanalysis of above
Cu	Mughrabi et al. (1986) and Mughrabi (2006a,b)	Tension		+0.4	-0.1	X-ray peak asymm.		Unloaded [001] oriented single crystal
Cu	Lepinoux and Kubin (1985)	Cyclic	Saturation w/ PSBs	+2.5	-0.5	In-situ TEM	RT	Loaded single crystal
Cu	Kassner et al. (2000)	Cyclic	Pre-sat. no PSBs	0	0	CBED	RT	Unloaded [123] single crystal
Cu	Kassner et al. (2000)	Cyclic	Pre-sat. no PSBs	0	00	Dipole sep.	RT	Unloaded [123] single crystal
Cu	Kassner et al. (2009)	Cyclic	Pre-sat. no PSBs	0	0	X-ray microbeam	RT	Unloaded [123] single crystal
Cu	Borbély et al. (2000)	Creep	Steady-state	+1.0	-0.08	X-ray peak asymm.	527 K	Loaded
Cu	Kassner et al. (2002)	Creep	steady-state	0	0	CBED	823 K	Unloaded
Cu	Straub et al. (1996)	Compression		-0.3- -0.6	+0.05- 0.08	X-ray peak asymm.	RT- 633 K	
Cu	Straub et al. (1996)	Compression		-	Observed	CBED	RT- 633 K	
Cu	Levine et al. (2006)	Tension		-	-0.17	X-ray microbeam	RT	Unloaded [001] oriented single crystal
Cu	Levine et al. (2006)	Compression (ave)		-	+0.29	X-ray microbeam theoretical/ X-ray	RT	Unloaded [001] oriented single crystal
Cu	Vogerand and Blum (1990)	Creep		5-7			527 K	
Cu	Levine et al. (2011)	Compression (ave)		-0.1	0.1	X-ray microbeam	RT	Unloaded [001] oriented single crystal
Si	Legros et al. (2008)	Cyclic (pre saturation)		0	0	CBED	RT	Unloaded
Ni	Hecker et al. (1997)	Cyclic	Saturation w/ PSBs	1.4-1.8	0.16-0.2	X-ray peak asymm.	RT	Loaded
Ni	Hecker et al. (1997)	Cyclic	Pre-sat. wo/ PSBs	0	0	X-ray peak asymm.	RT	Loaded
Al	Kassner et al. (1997, 2000)	Cyclic	Pre-sat wo/ PSBs	0	0	Dipole separation	77 K	Unloaded [123] oriented single crystal
Al	Kassner et al. (2002)	Creep	Steady-state	0	0	CBED	664 K	Unloaded
Al 5% Zn	Morris and Martin (1984)	Creep	Steady-state	+25	+1	Disl loops from precipitation pinning	483- 523 K	
-	Sedlacek et al. (2002)	Creep		1.5-10.0	0.5-1.0	Theoretical	Creep	
-	Gibeling and Nix (1980), Nix and Ilshner (1980)	Creep		7.7	~0.1-- 0.2	Theoretical	Creep	

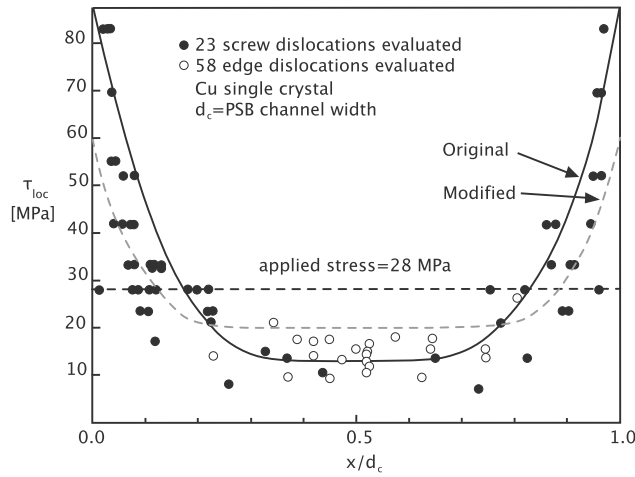


Fig. 12. Dislocation loop-radii-calculated LRIS from TEM thin foils extracted from neutron irradiated cyclically-deformed Cu single crystals (under load) with persistent slip bands (PSBs). From (Mughrabi, 1983) with recent modifications by the same investigators (Mughrabi and Pschenitzka, 2005) (dashed line). The high local stresses correspond to high dislocation density regions (PSB walls).

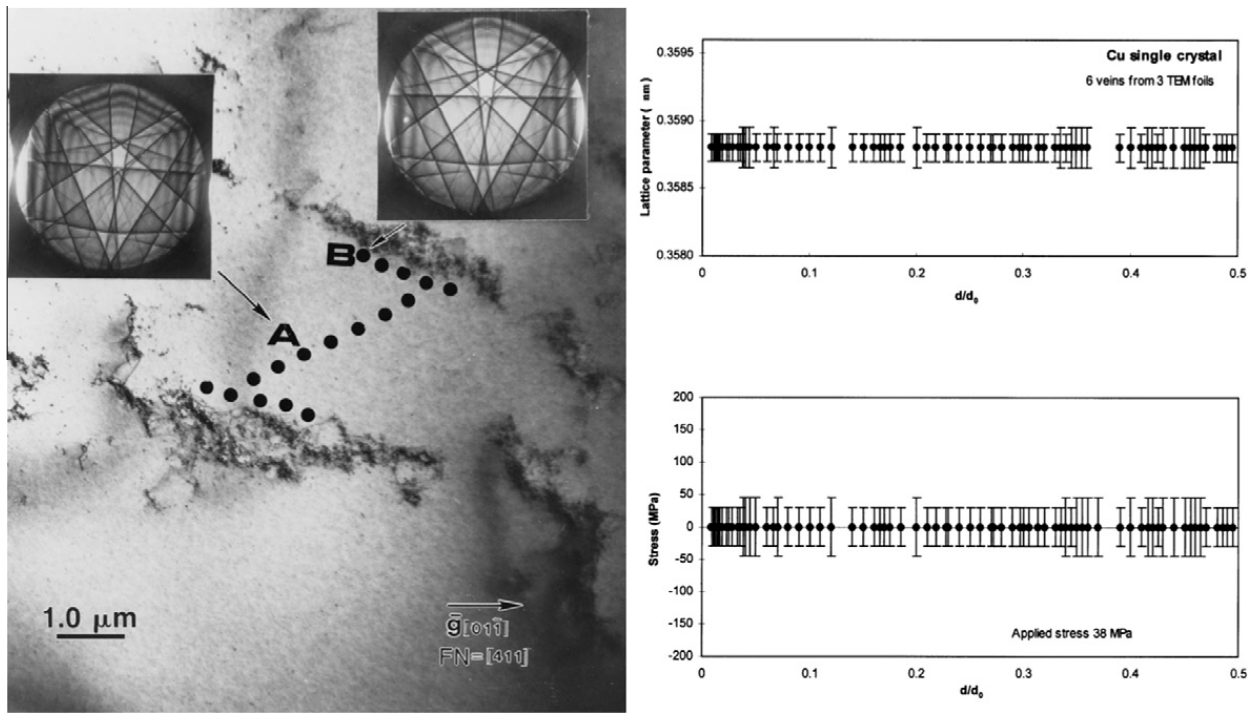


Fig. 13. TEM micrograph of a dipole channel and dipole-bundle walls (cyclic deformation to presaturation). Locations are indicated where CBED was used to determine the lattice parameter in order to assess any long-range internal stress. These black dots also project the area of the volume of material from which the CBED determinations were made. The specimen was oriented for single slip and deformed with low stress amplitudes to about half the saturation stress.

walls), cell walls or subgrain boundaries with high local-stresses. The second peak in deformed metals represents the lower dislocation density material (e.g., cell interiors) where the long range internal stresses are smaller than the applied stress. This asymmetry was illustrated in Fig. 7 where monotonic deformation was discussed. Asymmetry analysis varies, but PSB walls in cyclically deformed metals exhibit especially high stress values (i.e., LRIS = 1.4 σ_A to 1.8 σ_A). The earlier value of LRIS = 1.0 σ_A , ultimately suggested by Mughrabi, falls somewhat outside this range.

2.3.2. Multiple cycles: pre-saturation

2.3.2.1. Dipole height measurements. Prior to saturation of the flow stress, cyclically deformed metals harden, often without the formation of PSBs that are observed in saturation. Rather, there is a uniform “vein” substructure, where higher dislocation density (over a factor of 10) dipole bundles are evident (Basinski and Basinski, 1992; Laird, 1983). PSB walls, discussed in

the previous section, generally have higher dislocation densities than veins. The measurement of *maximum* dipole heights may allow the prediction of local stresses in cyclically deformed materials. The approximate stress to separate a dipole of height h_c can be calculated from the elastically isotropic equation:

$$\tau_d = \frac{Gb}{8\pi(1-\nu)h_c} \quad (6)$$

where G is the shear modulus, b the magnitude of the Burgers vector, and ν is Poisson's ratio. Wider separation dipoles than h_c are unstable under the local stress, τ . Cyclic deformation experiments on aluminum and copper single crystals (oriented for single slip) and deformed to about half the saturation stress by Kassner and Wall (1999) showed that the *average* dipole heights in the presaturation microstructure are also approximately *independent of location*, being equal in the dipole bundles (or veins) and the channels, consistent with other Ni work (Tippelt et al., 1997; Bretschneider et al., 1997) with PSBs. This suggests a uniform stress state across the microstructure (i.e. no LRIS). The maximum dipole height translates to a stress, according to Eq. (6), that is about *equal* to the applied (cyclic) stress for Al. This is shown in Table 2. Hence, this is evidence of an absence of any long-range internal stress in Al single crystals cyclically deformed to presaturation. However, the stress

Table 2

Three single crystals cyclically deformed to pre-saturation Al and Cu and saturation (Ni). Dipole heights were measured using TEM. Observed (τ_a) stresses and calculated (τ_d from Eq. (6)) stresses based on observed primary “ h ” values at ambient temperature and 77 K (Kassner et al., 2000).

	h (nm)		T/T_m	τ_d	τ_a	SFE (mJ/m)
Al	9.6	(ave)	0.12	51	20	200
(77 K)	31.0	(max) (h_c)		16	20	
Ni	4.1	(ave)	0.1	280	50	130
	5.7	(max) (h_c)	7	196	50	
Cu	5.2	(ave) Primary	0.2	132	19	60
	13.5	(max) Primary (h_c)	2	52	19	

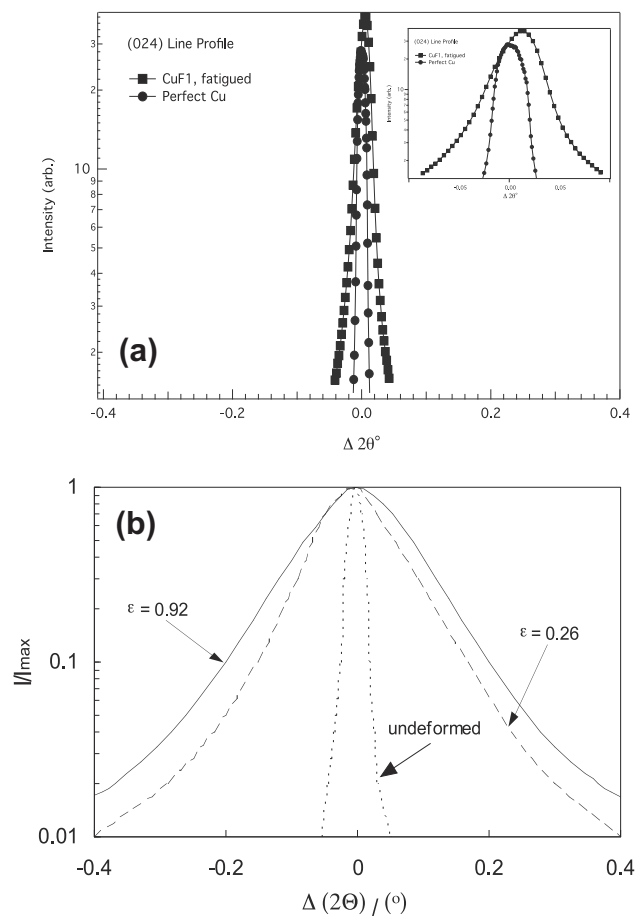


Fig. 14. (a) Spatially integrated 024 X-ray diffraction line profiles measured on the fatigued copper single crystal (presaturation) and on a non-deformed copper reference sample. (b) Fig. 7 shown for comparison.

to separate the widest dipoles is 2–3 times larger in Cu while for Ni it is within a factor of four (Kassner and Wall, 1999; Tippelt et al., 1997; Bretschneider et al., 1997; Kassner et al., 2000). The dipole heights are not expected to change significantly after unloading. Dislocation pile-ups (just a few dislocations) in the lower stacking fault energy Cu and Ni may explain narrower dipoles. Overall, these results are somewhat ambiguous in terms of an assessment of the magnitude of LRIS.

2.3.2.2. CBED. Lattice parameter measurements were made near (within 80 nm) dipole bundles and within the channels in Cu cyclically deformed to presaturation. These measurements lead to calculation of the stress (i.e. LRIS) in the unloaded TEM foil. No evidence of long-range internal stress was noticed. The uncertainty, however, was equal to the flow stress for the cyclically deformed Cu examined. Recent CBED work by Legros et al. (2008) on silicon deformed cyclically to presaturation also failed to detect LRIS to within 14% of the applied stress. Of course, one difficulty with these experiments is that the region of the foils examined in CBED is thin, under 100 nm, so relaxation of LRIS could have occurred in the unloaded specimens.

2.3.2.3. X-ray peak asymmetry in presaturation cyclic deformation. Investigators (Hecker et al., 1997; Biermann et al., 1993) have unloaded their samples from various points in the hysteresis loop to obtain X-ray asymmetry results on single-crystal Ni, and polycrystalline Cu. An interesting phenomenon is the observation of asymmetry for saturation (PSBs) as discussed earlier, but an absence for presaturation (no PSBs). This led Hecker et al. (1997) and Bretschneider (1998) to conclude the presence of LRIS only when PSBs are present in cyclically deformed Ni. This is consistent with the Kassner et al. (2000) and Legros et al. (2008) work on LRIS in cyclically deformed, pre-saturation, microstructures, and the DAXM work discussed below.

Microdiffraction experiments, as with monotonically deformed specimens, were performed on the cyclically deformed Cu single crystals of Fig. 13. The specimen was scanned in directions perpendicular to the dipole bundles (e.g., 220) to multiple channel widths. As a consequence, lattice parameter measurements are expected to be extracted from *both* the high dislocation density veins (dipole bundles) and channels. The dislocation densities in the dipole bundles and channels were $1.3 \times 10^{15} \text{ m}^{-2}$ and $8.3 \times 10^{12} \text{ m}^{-2}$ respectively (total dipole dislocation line-length per unit volume). The scans revealed no changes in the lattice parameter to within the uncertainty of $\pm 10^{-4}$. This uncertainty translates to a maximum stress $\cong E_{123} \times 10^{-4} = 13.1$ or a maximum LRIS about 0.34 the applied stress. Fig. 14 suggests some asymmetry in presaturation substructures on an “expanded scale” (see inset), although microbeam work did not notice any LRIS. However, some asymmetry (e.g. 10%) may originate from sources other than LRIS (Gaal, 1984), such as dislocation polarization (Delos-Reyes et al., 2003). Thus at least some of the asymmetry of the presaturation structure could be non-LRIS in origin.

3. Roadmap for the future

In summary, the concept of long range internal stresses has been with the mechanics and materials community, in some form, for over a hundred years, from the observation of the Bauschinger effect, the Mott–Seeger pile-up model, the composite model to experimental refinement up to the present day. Most (but not all) investigators subscribe to the validity of the internal stresses. The question has largely been the magnitude of the stress associated with various kinds of microstructures. About 30 years ago, the estimates were really very large; sometimes the values exceed 20 times the applied stress, with “typical” values for proposed LRIS being about a factor of 2–8 times larger than the applied stress. Over the subsequent 10 years, these estimates dramatically decreased with individual investigators sometimes decreasing their earlier values by a factor of two. Over the past 5 years or so, improved techniques using convergent beam electron diffraction (CBED) and X-ray microbeams at synchrotrons suggested that the examined microstructures (cyclic deformation to pre-saturation and 100-oriented Cu single crystals) have relatively low average LRIS (0–0.1 the applied stress). However, important questions remain.

In particular, the microstructures reliably and recently examined of low LRIS were also particularly non-complicated (dipole veins and low misorientation cell walls). It makes sense to examine those structures for which LRIS have been suggested to be relatively high. These include persistent slip band (PSB) walls and more complicated dislocation boundaries with higher misorientation [e.g. geometric necessary boundaries (GNBs)]. More complicated boundaries could also include severe plastic deformation (SPD) high angle boundaries for which indirect evidence (TEM image contrast) suggests the possibility of relatively high LRIS. While these are excellent avenues for study, some complications exist. X-ray microbeams currently resolve the stress within individual cell interiors and cell walls, which is an impressive accomplishment, but the strain measurements are only resolved for a single direction. This technique has not yet been able to assess the full strain tensor. Although this was acceptable for Cu single crystals under uniaxial loading along the [100] direction, more complicated dislocation structures such as those just described will benefit from the assessment of the full tensor. This will allow an assessment of the LRIS in a full assortment of microstructures and loading conditions. The authors believe this can be accomplished through a series of experimental refinements.

Another issue that must be raised regarding the two elite techniques of CBED and the X-ray microbeams is the fact that, currently, they are being performed on *unloaded* specimens. As discussed earlier, although it appears that the majority of the LRIS is “locked in” upon unloading, this should be additionally verified. This might be accomplished by *in situ* X-ray testing of loaded and subsequently unloaded specimens. *In situ* deformation experiments in CBED or X-ray microbeams may be prohibitively difficult. However, the recent work using X-ray microbeams confirmed that the conventional diffraction techniques by Ungar and co-workers discussed in earlier sections could be reliably utilized for this purpose. The X-ray peak

asymmetry that they noted does, in fact, result largely from LRIS and can be used to assess any diminution of the LRIS with unloading.

A verification for the dislocation basis of the LRIS that is consistent with the observations is critical. The composite model predicts higher local (LRIS) stresses in association with higher local dislocation densities. With the disparity in yield stress, dislocations accumulate at the interface for compatibility, producing a net dipole moment and thus dipolar LRIS. LRIS can arise from a summation of the stress fields of individual dislocations in a GNB cell wall or subgrain wall. It would make some sense to eventually model the LRIS as the summation of the stress fields of dislocations based on TEM images. Additionally, along similar lines, the Orowan–Sleeswyk model for the Bauschinger effect should be verified by dislocation dynamics models. The Orowan–Sleeswyk model does not rely on LRIS as a significant contributor for the principal features of the stress versus strain behavior with loading reversals.

Acknowledgments

M.E.K. acknowledges support from the NSF under Grant DMR-901838 Use of the Advanced Photon Source, an Office of Science User Facility operated for the US Department of Energy (DOE) Office of Science by Argonne National Laboratory, was supported by the US DOE under Contract No. DE-AC02-06CH11357.

References

- Argon, A.S., Takeuchi, S., 1981. Internal stresses in power-law creep. *Acta Metall.* 29, 1877.
- Basinski, Z.S., Basinski, S.J., 1992. Fundamental aspects of low amplitude cyclic deformation in face-centered cubic crystals. *Prog. Mater. Sci.* 36, 89–148.
- Biermann, H., Ungar, T., Pfannenmüller, T., Hoffmann, G., Borbély, A., Mughrabi, H., 1993. Local variations of lattice parameter and long-range internal stresses during cyclic deformation of polycrystalline copper. *Acta Metall. Mater.* 41, 2743–2753.
- Blum W., 2012. Personal Communication.
- Borbély, A., Hoffmann, G., Aernoudt, E., Ungar, T., 1997. Dislocation arrangement and residual long-range internal stresses in copper single crystals at large deformations. *Acta Mater.* 45, 89–98.
- Borbély, A., Blum, W., Ungar, T., 2000. On the relaxation of the long-range internal stresses of deformed copper upon unloading. *Mater. Sci. Eng.* 276, 186–194.
- Bretschneider, J., Holste, C., Tippelt, B., 1997. Cyclic plasticity of nickel single crystals at elevated temperatures. *Acta Mater.* 45, 3775–3783.
- Bretschneider, J., 1998. Private communication. Grenada, Spain.
- Delos-Reyes, M.A., Kassner, M.E., Levine, L.E., 2003. X-ray diffraction and the existence of long-range internal stresses. In: Kahn, A.S., Kazmi, R., Zhou, J. (Eds.), *Dislocations, Plasticity and Metal Forming*. Neat Press, Fullerton, MD, p. 264.
- Gaal, I., 1984. In: Hessel Andersen, N., Eldrup, M., Hansen, N., Juul Jensen, D., Leffers, T., Lilholt, H., Pedersen, O.B., Singh, B.N. (Eds.), *Proc. Fifth Riso Int. Symp. on Metallurgy and Mat. Sci.* Riso Nat. Lab, Roskilde, DK, pp. 249–254.
- Gibeling, J.C., Nix, W.D., 1980. A numerical study of long range internal stresses associated with subgrain boundaries. *Acta Metall.* 28, 1743–1752.
- Gibeling, J.C., Nix, W.D., 1981. Observations of anelastic backflow following stress reductions during creep of pure metals. *Acta Metall.* 29, 1769.
- Groma, I., 1998. X-ray line broadening due to an inhomogeneous dislocation distribution. *Phys. Rev. B* 57, 7535–7542.
- Hansen, N., 1999. Private Communication. Cincinnati, OH.
- Hecker, M., Thiele, E., Holste, C., 1997. X-ray diffraction analysis of internal stresses in the dislocation structure of cyclically deformed nickel single crystals. *Mater. Sci. Eng.* A234–236, 806–809.
- Jakobsen, B., Poulsen, H.F., Lienert, U., Almer, J., Shastri, S.D., Sørensen, H.O., Gundlach, C., Pantleon, W., 2006. Formation and subdivision of deformation structures during plastic deformation. *Science* 32, 889–892.
- Kassner, M.E., Ziaai-Moayyed, A.A., Miller, A.K., 1985. Some trends observed in the elevated-temperature kinematic and isotropic hardening of type 304 stainless steel. *Metall. Trans.* 16A, 1069–1076.
- Kassner, M.E., 1989. The rate dependence and microstructure of high-purity silver deformed to large strains between 0.16 and 0.30T_m. *Metall. Trans.* 20, 2001–2010.
- Kassner, M.E., Wall, M.A., Sleeswyk, A.W., 1991. Some observations during in-situ reversed deformation of aluminum single crystals in the HVEM using the X–Y method. *Scripta Metall. Mater.* 25, 1701–1706.
- Kassner, M.E., McQueen, H.J., Pollard, J., Evangelista, E., Cerri, E., 1994a. Restoration mechanisms in large-strain deformation of high purity aluminum at ambient temperature. *Scripta Metall. Mater.* 31, 1331–1336.
- Kassner, M.E., Pollard, J., Evangelista, E., Cerre, E., 1994b. Restoration mechanisms in large-strain deformation of high purity aluminum at ambient temperature and the determination of the existence of “steady-state”. *Acta Metall. Mater.* 42, 3223–3230.
- Kassner, M.E., Wall, M.A., Delos-Reyes, M.A., 1997. Microstructure and mechanisms of cyclic deformation of aluminum single crystals at 77 K. *Metall. Mater. Trans.* 28A, 595–609.
- Kassner, M.E., Wall, M.A., 1999. Microstructure and mechanisms of cyclic deformation in aluminum single crystals at 77 K: Part II. Edge dislocation dipole heights. *Metall. Mater. Trans.* 30A, 777–779.
- Kassner, M.E., Perez-Prado, M.-T., Vecchio, K.S., Wall, M.A., 2000. Determination of internal stresses in cyclically deformed Cu single crystals using CBED and dislocation dipole separation measurements. *Acta Mater.* 48, 4247–4254.
- Kassner, M.E., Perez-Prado, M.T., Long, M., Vecchio, K.S., 2002. Dislocation microstructure and internal-stress measurements by convergent-beam electron diffraction on creep-deformed Cu and Al. *Metall. Mater. Trans.* 33A, 311–318.
- Kassner, M.E., Geanti, P., Levine, L.E., Larson, B.C., 2009. Long range internal stresses in monotonically and cyclically deformed single crystals. *Int. J. Mater. Res.* 100, 33.
- Kassner, M.E., 2009. *Fundamentals of Creep in Metals and Alloys*. Elsevier, Oxford.
- Khan, S.M.A., Zbib, H.M., Hughes, D.A., 2004. Modeling planar dislocation boundaries using multi-scale dislocation dynamics plasticity. *Int. J. Plasticity* 20, 1059.
- Krivoglaž, M.A., Ryaboshapka, K.P., 1963. Order–disorder phenomena in alloys. *Phys. Met. Metall.* 12, 465.
- Kuhlmann-Wilsdorf, D., 1999. Deformation bands, the LED theory and their importance in texture development: Part II. Theoretical conclusions. *Metall. Mater. Trans.* 30A, 2391.
- Laird, C., 1983. In: Nabarro, F.R.N. (Ed.), *Dislocations in Solids*, vol. 6. North Holland, pp. 1–120.
- Larson, B.C., Yang, W., Ice, G.E., Budai, J.D., Tischler, J.S., 2002. Three-dimensional X-ray structural microscopy with submicrometre resolution. *Nature* 415, 887–890.
- Legros, M., Ferry, O., Houdellier, F., Jacques, A., George, A., 2008. Fatigue of single crystalline silicon: mechanical behaviour and TEM observations. *Mater. Sci. Eng.* A483–484, 353–364.

- Lepinoux, J., Kubin, L.P., 1985. In situ TEM observations of the cyclic dislocation behaviour in persistent slip bands of copper single crystals. *Philos. Mag.* 57, 675–696.
- Levine, L.E., Larson, B.C., Yang, W., Kassner, M.E., Tischler, J.Z., Delos-Reyes, M.A., Fields, R.J., Liu, W., 2006. X-ray microbeam measurements of individual dislocation cell elastic strains in deformed single-crystal copper. *Nat. Mater.* 5, 619–622.
- Levine, L.E., Geantil, P., Larson, B.C., Tischler, J., Kassner, M.E., Liu, W., Stoudt, M.R., Tavazza, F., 2011. Impact of dislocation cell elastic strain variations on line profiles from deformed copper. *Acta Mater.* 59, 5803–5811.
- Levine, L.E., Geantil, P., Larson, B.C., Tischler, J.Z., Kassner, M.E., Liu, W., 2012. Validating classical line profile analyses using microbeam diffraction from individual dislocation cell walls and cell interiors. *J. Appl. Cryst.* 45, 157–165.
- McQueen, H.J., Blum, W., Straub, S., Kassner, M.E., 1993. Dynamic grain growth: a restoration mechanism in 99.999 Al. *Scripta Metall. Mater.* 28, 1299–1304.
- Morris, M.A., Martin, J.L., 1984. Evolution of internal stresses and substructure during creep at intermediate temperatures. *Acta Metall.* 32, 1609–1623.
- Mott, N.F., 1952. A theory of work-hardening of metal crystals. *Philos. Mag.* A 43, 1151.
- Mughrabi, H., 1983. Dislocation wall and cell structures and long-range internal stresses in deformed metal crystals. *Acta Metall.* 31, 1367–1379.
- Mughrabi, H., Ungar, T., Kienle, W., Wilkens, M., 1986. Long-range internal stresses and asymmetric X-ray line-broadening in tensile-deformed [001]-orientated copper single crystals. *Philos. Mag.* A 53, 793–813.
- Mughrabi, H., 1987. A two-parameter description of heterogeneous dislocation distributions in deformed metal crystals. *Mater. Forum* 10, 1.
- Mughrabi, H., Ungar, T., 2002. Long range internal stresses in deformed single-phase materials: the composite model and its consequences. *Dislocations in Solids*. Elsevier, Amsterdam, p. 345.
- Mughrabi, H., Pschenitzka, F., 2005. Constrained glide and interaction of bowed-out screw dislocations in confined channels. *Philos. Mag.* 85, 3029–3045.
- Mughrabi, H., 2006a. Deformation-induced long-range internal stresses and lattice plane misorientations and the role of geometrically necessary dislocations. *Philos. Mag.* A 86, 4037–4054.
- Mughrabi, H., 2006b. Dual role of deformation-induced geometrically necessary dislocations with respect to lattice plane misorientations and/or long-range internal stresses. *Acta Mater.* 54, 3417–3427.
- Nabarro, F.R.N., de Villiers, H., 1995. *Physics of Creep*. Taylor and Francis, Belfast.
- Neumann, P., 1999. Private Communication. San Diego, CA.
- Nix, W.D., Ilshner, B., 1980. Mechanisms controlling creep of single phase metals and alloys. In: Haasen, P., Gerold, V., Kosterz, G. (Eds.), *Strength of Metals and Alloys*. Pergamon Press, Oxford, p. 1503.
- Orowan, E., 1959. Causes and effects of internal stresses. In: Rassweiler, G.M., Grube, W.L. (Eds.), *Internal Stresses and Fatigue in Metals*. General Motors Symposium. Elsevier, Amsterdam, pp. 59–80.
- Pantleon, W., Poulsen, H., Almer, J., Lienert, U., 2004. In situ X-ray peak shape analysis of embedded individual grains during plastic deformation of metals. *Mater. Sci. Eng.* 387–389A, 339–342.
- Pedersen, O., Brown, L., Stobbs, W., 1981. The Bauschinger effect in copper. *Acta Metall.* 29, 1843–1850.
- Schafner, E., Simon, K., Bernstorff, S., Hanak, P., Tichy, G., Ungar, T., Zehetbauer, M.J., 2005. A second-order phase-transformation of the dislocation structure during plastic deformation determined by in situ synchrotron X-ray diffraction. *Acta Mater.* 53, 215–322.
- Sedlacek, R., Blum, W., Kratochvil, J., Forest, S., 2002. Subgrain formation during deformation: physical origin and consequences. *Metall. Mater. Trans.* 33A, 319–327.
- Seeger, A., Diehl, J., Mader, S., Rebstock, H., 1957. Work-hardening and work-softening of face-centred cubic metal crystals. *Philos. Mag.* 2, 323–350.
- Sleeswyk, A.W., James, M.R., Plantinga, D.H., Maathius, W.S.T., 1978. Reversible strain in cyclic plastic deformation. *Acta Metall.* 26, 1265–1271.
- Straub, S., Blum, W., Maier, H.J., Ungar, T., Borbély, A., Renner, H., 1996. Long-range internal stresses in cell and subgrain structures of copper during deformation at constant stress. *Acta Mater.* 44, 4337–4350.
- Thiehnsen, K.E., Kassner, M.E., Pollard, J., Hiatt, D.R., Bristow, B.M., 1993a. The effect of nickel, chromium, and primary. *Metall. Trans.* 24, 1819–1826.
- Thiehnsen, M.E., Kassner, M.E., Hiatt, D.R., Bristow, B., 1993b. Titanium 92. TMS, Warrendale, PA, pp. 1717–1724.
- Tippelt, B., Bretschneider, J., Hahner, P., 1997. The dislocation microstructure of cyclically deformed nickel single crystals at different temperatures. *Phys. Stat. Sol. A* 163, 11–26.
- Ungar, T., Mughrabi, H., Rönnpagel, D., Wilkens, M., 1984. X-ray line-broadening study of the dislocation cell structure in deformed [001]-orientated copper single crystals. *Acta Metall.* 32, 333.
- Ungar, T., Mughrabi, H., Wilkens, M., Hilscher, A., 1991. Long-range internal stresses and asymmetric X-ray line-broadening in tensile-deformed [001]-oriented copper single crystals: the correction of an erratum. *Philos. Mag.* A 64, 495–496.
- Vogerand, S., Blum, W., 1990. In: Wilshire, B., Evans, R.W. (Eds.), *Fracture of Engineering Materials and Structures*. Inst. Metals, London, pp. 67–79.
- Weertman, J., Weertman, J.D., 1992. *Elementary Dislocation Theory*. Oxford Press, Oxford, p. 127.
- Wilkins, M., 1970. The determination of density and distribution of dislocations in deformed single crystals from broadened X-ray diffraction profiles. *Phys. Stat. Sol. A* 2, 359–370.
- Yan, J., 1998. Study of the Bauschinger effect in various spring steels. Thesis, Univ. Toronto, Dept. Metallurgy and Materials Sci.